Geothermics 121 (2024) 103021

Contents lists available at ScienceDirect

Geothermics

journal homepage: www.elsevier.com/locate/geothermics

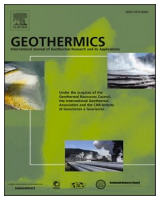

Sequential long-term optimization of shallow geothermal systems under descriptive uncertainty and dynamic variation of heating demand

Hesam Soltan Mohammadi [a,*], Lisa Maria Ringel [a], Michael de Paly [b], Peter Bayer [a]

[a] Department of Applied Geology, Institute of Geosciences and Geography, Martin Luther University Halle-Wittenberg, von-Seckendorff-Platz 3, 06120 Halle (Saale), Germany

[b] 5Minds IT-Solutions, De-la-Chevallerie-Straße 42-44, 45894 Gelsenkirchen, Germany

ARTICLE INFO

Keywords:
Low-enthalpy geothermal energy
Closed-loop
Mathematical optimization
Uncertainty

ABSTRACT

Unmanaged heat extraction, as well as the adjacency of multiple borehole heat exchangers (BHEs) in a field, can lead to undesirable thermal conditions in the ground. The failure to properly control induced thermal anomalies is perceived as a severe risk to closed-loop geothermal systems, as the detrimental effects on the ground can substantially deteriorate performance or nullify the compatibility of an operating system with regulatory mandates. This paper presents a flexible framework for the combined simulation-optimization of BHE fields during the entire lifespan. The proposed method accounts for the uncertainties in subsurface characteristics and energy consumption in order to minimize the temperature change caused by the heat extraction during the operation. The descriptive uncertainty is introduced as a deviation of the monitored temperature from the simulated temperature change, whereas the variation of the energy demand appears as over- or under-consumption against the scheduled demand. The presented new sequential procedure, by updating the thermal conditions of the ground with temperature measurements, continuously executes the optimization during the operation period and enables the generation of revised load distributions. In this study, two fields with five and 26 BHEs are considered to demonstrate the performance of the proposed method. Sequential optimization outperforms single-step optimization by providing the basis for more strategic load-balancing patterns and yielding lower temperature anomalies of about 2.9 K and 8.9 K in each BHE configuration, respectively, over 15 operational years.

1. Introduction

Environmental concerns, climate change, and global energy crisis are all among the reasons that compel us to use renewable energy resources. In recent decades, shallow geothermal energy has emerged as one of the potential resources to achieve this goal, especially for heating and cooling purposes. Worldwide, geothermal resources provided approximately 108,000 MW of thermal energy in 2019 for 88 countries, representing a growth of about 52 % compared to 2014 (Lund and Boyd, 2016; Lund and Toth, 2021). Shallow geothermal energy as an omnipresent resource can be accessed by means of drilling boreholes to a depth of a few tens of meters to a couple of hundred meters in the ground. The boreholes equipped with tubes are borehole heat exchangers (BHEs) that circulate a heat carrier fluid connected with an aboveground heat pump to supply a given heating (or cooling) demand (Gil et al., 2020). The energy supplied by a BHE for a given time can be termed as "load".

Since the subsurface thermal processes are normally slow, unmanaged energy harvesting can yield undesired local cooling, and in the worst case trigger thermal shocks that the ground cannot fully dissipate. Imbalanced operation of multiple BHEs or disproportionate extraction or injection can cause environmental and technical issues that may jeopardize the efficiency and even the feasibility of operation. Exemplifying this issue, Chen et al. (2021) have assessed the underperformance of a field of 56 BHEs in Leicester, UK, by comparing numerical simulation with monitoring data. They found that the studied BHE field can be efficiently operated for a maximum of 20 years under the designed scenario due to heat accumulation in the central BHEs. In addition to a potential technical malfunction, long-term performance of BHE systems can result in subsurface thermal anomalies that violate local environmental regulations. In most countries with geothermal plants (Blum et al., 2021; Gil and Moreno, 2020; Haehnlein et al., 2010; Tsagarakis et al., 2020), there is a defined maximum threshold for the tolerable induced temperature anomalies in the ground, which is the basis for the design and operation of such systems.

* Corresponding author.
E-mail address: hesam.soltan-mohammadi@geo.uni-halle.de (H. Soltan Mohammadi).

https://doi.org/10.1016/j.geothermics.2024.103021
Received 12 July 2023; Received in revised form 2 April 2024; Accepted 14 April 2024
Available online 9 May 2024
0375-6505/© 2024 The Authors. Published by Elsevier Ltd. This is an open access article under the CC BY-NC-ND license (http://creativecommons.org/licenses/by-nc-nd/4.0/).

Nomenclature

x	Coordinate in x-direction (m)
y	Coordinate in y-direction (m)
z	Coordinate in z-direction (m)
r	Distance to the BHE axis (m)
$\varkappa$	Auxiliary variable
L	Length of borehole (m)
N_{BHE}	Number of BHEs
N_t	Number of time steps
$N_{t_{opt}}$	Number of optimization time steps
t	Time (s)
S	Field domain
q	Heat extraction/injection rate (Wm^{-1})
T	Temperature (K)
ΔT	Temperature change (K)
ω	Thermal response coefficient (-)
λ	Thermal conductivity ($W\ m^{-1}\ K^{-1}$)
E	Energy demand (W)
α	Thermal diffusivity ($m^2\ s^{-1}$)
w	Weighting factor (-)
$\vec{e}$	All-ones vector

Subscripts

k	Counter index of N_{BHE}
l	Counter index of N_t
m	Counter index of $N_{t_{opt}}$
i	Counter index of x
j	Counter index of y
meas	Measured
sim	Simulated
DU	Descriptive uncertainty

To counteract the shortcomings in the performance of BHE fields and to mitigate the thermal anomalies, accurate subsurface characterization and simulation of the long-term system performance are needed. In order to properly design and operate BHE systems, it is crucial to have a thorough knowledge of the thermal properties of the ground, such as thermal conductivity and borehole resistivity (Erol and François, 2014; Heim et al., 2022; Hein et al., 2016). The most straightforward approach in practice for obtaining these parameters is to conduct in-situ measurements such as the thermal response test (TRT) (Gehlin, 2002; Spitler and Gehlin, 2015). Given that TRTs are local measurements over a short period of time before the start of operation, they only examine the in-situ conditions in the vicinity of a borehole and they cannot resolve characteristic subsurface heterogeneities (Boban et al., 2020; Lee, 2011; Luo et al., 2014; Pasquier et al., 2019; Raymond and Lamarche, 2013; Wagner et al., 2012; Zhang et al., 2022). Aside from this, multiple further factors influence the performance of BHEs such as groundwater flow (Antelmi et al., 2023; Previati and Crosta, 2024; Signorelli et al., 2007; Zanchini et al., 2012), surface water bodies (Perego et al., 2022), ground-surface thermal coupling (Bidarmaghz et al., 2016; Nguyen et al., 2017), seasonal variations and consumer behavior (Yoshioka et al., 2022), and the type or the arrangement of BHEs (Zhang et al., 2021). This limited predictability of the system's performance over the operational lifespan motivates the use of optimization and control techniques. The concept of individual load optimization in a BHE field was introduced by Beck et al. (2010), and it was further developed to also consider groundwater (Hecht-Méndez et al., 2013). Beck et al. (2013) suggested a procedure for optimal BHE positioning and allocation of loads, and this was modified to detect the least effective BHEs and put them out of service (Bayer et al., 2014). Several alternative solutions have been presented to optimize irregular BHE spacing and minimize their numbers while fulfilling a given energy demand (Cimmino and Bernier, 2014; Egidi et al., 2023; Spitler et al., 2020; Spitler et al., 2022; Noël and Cimmino, 2022). Notwithstanding, these optimization concepts do not take into account the dynamics of the ground and possible uncertainties that may arise due to the interaction of multiple BHEs (Ma et al., 2020).

The general idea of optimal control techniques is to regularly monitor the ground during operation to provide an automated mechanism that compares the model-based simulations with the recorded data at specific time intervals (BniLam and Al-Khoury, 2020; Shoji et al., 2023). Some studies have presented several optimum operating scenarios, but the derived operational strategy is based on the comparison of a limited number of selected scenarios (Liu et al., 2015; Yavuzturk and Spitler, 2000; Zhou et al., 2016). Available control methods typically focus on applying dynamic programming, model predictive control, or artificial neural networks, while the adopted BHE and subsurface simulation models are often simplified (Atam et al., 2016; De Ridder et al., 2011; Gang et al., 2014). As pointed out by Ikeda et al. (2017), one of the main concerns with optimal control strategies is that the developed methodologies mostly fail to properly account for the thermal conditions and response of the ground.

The main motivation of this paper is to enhance the flexibility of combined simulation-optimization for computing the heating load patterns in order to efficiently prolong the operational life and simultaneously comply with regulatory requirements and environmental concerns. Although this study only focuses on cases with heating applications, the proposed framework is also applicable to cooling purposes. Our approach is to simultaneously monitor the subsurface temperature evolution and actual energy demand at the particular time steps to be able to update the subsurface thermal conditions for optimization of load balancing in an iterative framework. Hence, initial postulates and rough estimations are used to initialize the operation in an optimal way. A schematic illustration of our methodology is shown in Fig. 1. In the following, we first present the governing equations for the simulation of the temporal temperature change caused by multiple BHEs in a field. Thereafter, the objective function and the relevant optimization constraints are defined. For demonstration of the new proposed procedure, two theoretical case studies are developed, and in the next section, the maximum temperature changes in both fields are compared when single-step and sequential optimization are applied. The results

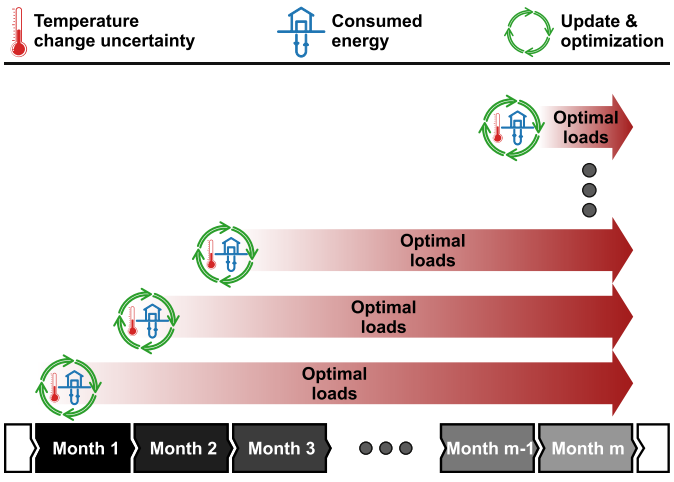

Fig. 1. Conceptual diagram of sequential optimization.

section proceeds with a comparative study on the optimal load distributions, and the capability of the new sequential optimization procedure to deal with uncertainties in energy demand is evaluated.

2. Methodology

2.1. Simulation of a borehole heat exchangers field

The spatial and temporal temperature change induced by a single BHE can be approximated by a finite line-source (FLS) model (Beck et al., 2013; Stauffer et al., 2013; Zeng et al., 2002):

$$\Delta T(q,\Delta x,\Delta y,\Delta z,t)=\frac{q}{4\pi\lambda}\left(\int_0^L\frac{1}{r}\operatorname{erfc}\left(\frac{r}{\sqrt{4\alpha t}}\right)dz'-\int_{-L}^0\frac{1}{r}\operatorname{erfc}\left(\frac{r}{\sqrt{4\alpha t}}\right)dz'\right) \tag{1}$$

This assumes conduction in a homogeneous and isotropic subsurface medium with properties that are independent of the temperature. In the equation, $\Delta T=T_\infty-T$ refers to the deviation from the ambient, unperturbed temperature distribution T_∞. Since we are only concerned with the evaluation of temperature change in this study and FLS assumes a uniform and undisturbed temperature at $t=0$ in the whole domain, the absolute value of T_∞ is not relevant for our study, and exclusively the temperature change is attributed to operation. L is the length of the borehole, λ is the thermal conductivity, α is the thermal diffusivity, and r represents the horizontal distance to the borehole axis Δx, Δy, and the vertical axis of a borehole $(z-z')$, such that $r=\sqrt{\Delta x^2+\Delta y^2+(z-z')^2}$. q is the heat flow rate per length of the borehole, which is a positive value in the case of heat extraction. If cooling is intended to be taken into account, this is realized by heat injection rather than extraction and is expressed by a negative sign.

The superposition principle can be applied to account for a set of boreholes $k=1,\cdots,N_{BHE}$ at locations (x_k,y_k) and a temporal variation of the load as a series of $l=1,\cdots,N_t$ load pulses $\vec{q}=(q_{1,1},\cdots,q_{N_{BHE},1},\cdots,q_{1,N_t},\cdots,q_{N_{BHE},N_t})^T$ for each borehole (Abdelaziz et al., 2014; Bernier et al., 2004; Cimmino et al., 2013; Cimmino and Bernier, 2014; Eskilson, 1987; Fascì et al., 2021; Lamarche, 2011; Lazzarotto, 2016; Lazzarotto and Björk, 2016; Marcotte et al., 2010; Marcotte and Pasquier, 2008; Michopoulos and Kyriakis, 2009). This leads to an estimation of the temperature change at any location relative to a borehole Δx_i, Δy_j at time t

$$\overrightarrow{\Delta T}\left(\vec{q},\Delta x_i,\Delta y_j,t\right)=\sum_{l=1}^{N_t}\sum_{k=1}^{N_{BHE}}q_{k,l}\;\omega_{k,l}\left(\Delta x_i,\Delta y_j,t\right) \tag{2}$$

with the response coefficient

$$\omega_{k,l}\left(\Delta x_i,\Delta y_j,t\right)=\frac{1}{4\pi\lambda}\left(\int_0^L\frac{1}{r}\operatorname{erfc}\left(\frac{r}{\sqrt{4\alpha(t-t_{l-1})}}\right)dz'-\int_{-L}^0\frac{1}{r}\operatorname{erfc}\left(\frac{r}{\sqrt{4\alpha(t-t_{l-1})}}\right)dz'-\int_0^L\frac{1}{r}\operatorname{erfc}\left(\frac{r}{\sqrt{4\alpha(t-t_l)}}\right)dz'+\int_{-L}^0\frac{1}{r}\operatorname{erfc}\left(\frac{r}{\sqrt{4\alpha(t-t_l)}}\right)dz'\right), \tag{3}$$

where t is the current time $t\geq t_l$ (Beck et al., 2013). Due to the assumption of temperature-independent parameters, the temperature distribution can be formulated as a linear problem

$$\overrightarrow{\Delta T}\left(\vec{q},\Delta x_i,\Delta y_j,t\right)=\vec{\omega}\left(\Delta x_i,\Delta y_j,t\right)\;\vec{q} \tag{4}$$

with $\vec{\omega}=(\omega_{1,1},\cdots,\omega_{N_{BHE},1},\cdots,\omega_{1,N_t},\cdots,\omega_{N_{BHE},N_t})$. As initial condition, $\overrightarrow{\Delta T}(\vec{q},\Delta x_i,\Delta y_j,t_0)=0$ holds for $t_0=0$.

2.2. Optimization objective

The optimization procedure we use here is adopted from the method that was proposed by De Paly et al. (2012). The objective is to avoid local ground temperature decline in the field by minimizing the maximum temperature change induced by all BHE operations. The underlying rationale is that the ground heat exchange is optimal when "cold" BHEs are avoided, and thus also the performance of the heat pump is indirectly optimized. In the mathematical formulation this means identifying the position in the considered region $\Delta x_i,\Delta y_j\in S$ where the maximum temperature change occurs, and distributing the loads temporarily and spatially such that the weighted sum of the maximum temperature change of the entire operation period and the timestep-wise maximum temperature change is minimized:

$$arg\min\left(w\cdot\max\left(\overrightarrow{\Delta T}\left(\vec{q},\Delta x_i,\Delta y_j,t_{N_t}\right)\right)+\sum_{l=1}^{N_t}\max\left(\overrightarrow{\Delta T}\left(\vec{q},\Delta x_i,\Delta y_j,t_l\right)\right)\right), \tag{5}$$

subject to

$$\begin{aligned}&E_l=\sum_{k=1}^{N_{BHE}}q_{k,l},\\&\Delta x_i,\Delta y_j\in S,\end{aligned} \tag{6}$$

for all $l=1,\ldots,N_t$. The first constraint ensures that the heat demand is met in each time step and the latter restricts the max-norm to the investigated region. N_t specifies the number of time segments l and thus defines the time resolution, e.g., for computation of daily or monthly changing optimal individual BHE loads. The first term in the objective function is of greater importance to us since the primary concern is to minimize the temperature change for the entire time period and not for individual time steps. To make this superiority explicit, a weighting factor w is defined that grants a higher weight to the first term. w is fixed at 100 in this study. If the entire operation time is discretized by l segments, and an optimal transient loading pattern is derived based on the given initial conditions at t_0 before the operation of the BHE field only, then we define this procedure as "single-step optimization".

2.3. Sequential optimization procedure

We investigate the potential to learn during BHE field operation. Most convenient is to re-run the optimization after a period of operation and take the prevailing ground thermal state as a new initial condition. In our application example, we study the case where the monthly extracted heat demand deviates from the predicted one. Furthermore, we assume that the line-source model is not exact due to simplifying assumptions on the ground thermal properties and processes. The resulting deviations between simulated and observed real thermal conditions in the ground are regularly inspected during the course of operation and the BHE loading strategy is optimized again.

For this purpose, the previously defined objective function (Eq. (5)) is reformulated such that the optimization problem can be posed and solved as linear problems by applying auxiliary virtual variables z_0 and z_l

$$\min\left(w\cdot x_0+\sum_{l=1}^{N_t}x_l\right), \tag{7}$$

subject to the constraints

$$\begin{aligned}
&\overrightarrow{\Delta T}\left(\vec{q},\Delta x_i,\Delta y_j,t_{N_t}\right)-x_0\vec{e}<0\\
&-\overrightarrow{\Delta T}\left(\vec{q},\Delta x_i,\Delta y_j,t_{N_t}\right)-x_0\vec{e}<0\\
&\overrightarrow{\Delta T}\left(\vec{q},\Delta x_i,\Delta y_j,t_l\right)-x_l\vec{e}<0\\
&-\overrightarrow{\Delta T}\left(\vec{q},\Delta x_i,\Delta y_j,t_l\right)-x_l\vec{e}<0\\
&E_l=\sum_{k=1}^{N_{BHE}}q_{k,l}\\
&\Delta x_i,\Delta y_j\in S,
\end{aligned} \tag{8}$$

for all $l=1,\cdots,\ N_t$. $\vec{e}$ denotes the vector of ones with N_{BHE} entries. The optimization is repeated iteratively for predefined timesteps t_m ($m=1,\cdots,N_{t_{opt}}$), which we call "sequential optimization".

Based on the actual extracted energy and the measured ground temperatures at each time step, the real-time subsurface temperature change, $\overrightarrow{\Delta T}_{meas}(\Delta x_i,\Delta y_j,t_{m-1})$, is determined, which differs from the model-based simulations, $\overrightarrow{\Delta T}_{sim}(\vec{q},\Delta x_i,\Delta y_j,t_{m-1})$. This real temperature change of the BHE field is considered as the most accurate starting point for the recalculation of the optimal load patterns of the upcoming months. The measured temperature is assumed to be a representative proxy for the current thermal response and conditions of the ground. The final outcome of the sequential optimization at each time step is a new load allocation, $\vec{q}$, for the individual boreholes in the remaining time steps. This sequential optimization is realized as a loop for $m=1,\cdots,N_{t_{opt}}$:

$$\min\left(w\cdot x_0+\sum_{l=m}^{N_t}x_l\right), \tag{9}$$

subject to

$$\begin{aligned}
&\overrightarrow{\Delta T}\left(\vec{q},\Delta x_i,\Delta y_j,t_{N_t}\right)-\overrightarrow{\Delta T}\left(\vec{q},\Delta x_i,\Delta y_j,t_{m-1}\right)-x_0\vec{e}<-\overrightarrow{\Delta T}_{meas}\left(\vec{q},\Delta x_i,\Delta y_j,t_{m-1}\right)\\
&-\overrightarrow{\Delta T}\left(\vec{q},\Delta x_i,\Delta y_j,t_{N_t}\right)+\overrightarrow{\Delta T}\left(\vec{q},\Delta x_i,\Delta y_j,t_{m-1}\right)-x_0\vec{e}<\overrightarrow{\Delta T}_{meas}\left(\vec{q},\Delta x_i,\Delta y_j,t_{m-1}\right)\\
&\overrightarrow{\Delta T}\left(\vec{q},\Delta x_i,\Delta y_j,t_l\right)-\overrightarrow{\Delta T}\left(\vec{q},\Delta x_i,\Delta y_j,t_{m-1}\right)-x_l\vec{e}<-\overrightarrow{\Delta T}_{meas}\left(\vec{q},\Delta x_i,\Delta y_j,t_{m-1}\right)\\
&-\overrightarrow{\Delta T}\left(\vec{q},\Delta x_i,\Delta y_j,t_l\right)+\overrightarrow{\Delta T}\left(\vec{q},\Delta x_i,\Delta y_j,t_{m-1}\right)-x_l\vec{e}<\overrightarrow{\Delta T}_{meas}\left(\vec{q},\Delta x_i,\Delta y_j,t_{m-1}\right)\\
&E_l=\sum_{k=1}^{N_{BHE}}q_{k,l}\\
&\Delta x_i,\Delta y_j\in S,
\end{aligned} \tag{10}$$

for all $l=m,\ldots,N_t$. In this loop, the simulated temperature change from previous timesteps is iteratively replaced with the actual measured temperature. For $m=1$, the results of the sequential and single-step optimization coincide. The flowchart of the proposed method is shown in Fig. 2.

2.4. Parameter settings of case studies

Two hypothetical case studies with different configurations of the BHE field are defined. In case study I, five BHEs, and in case study II, 26 BHEs are considered for layouts as shown in a top view in Fig. 3. The BHEs are located in a 35 m × 40 m and 50 m × 60 m area, respectively, where their positions are denoted by circles. The spacing between the BHEs is set to 5 m, which in practice may be sufficient to prevent strong thermal interference from adjacent boreholes (Gultekin et al., 2016; VDI 2001), but commonly long-term operation yields superpositioning of the thermal effects of neighboring BHEs (Rivera et al., 2017). Only conductive heat transfer to the BHEs is simulated based on Eq. (1), respecting a given time-dependent heat demand profile for an operating period of 15 years.

We account for inaccuracy in the models used to predict the ground temperatures of the two cases. It is assumed that the thermal response of the boreholes, which are represented by filled circles in Fig. 3, are prone to deviations from the simulation. In both case studies, the temperature change is calculated once before the start of operation using Eq. (1) for all time steps and considered as a prior value. At each time step, the simulated temperature change is compared to the measured temperature (Eq. (10)). To construct a virtual reality that resembles the measured temperature, an uncertainty percentage is assumed at the location of each borehole. Fig. 3 shows the assumed distribution of the uncertainty rates in both fields, and the structure of this variation can be attributed to local heterogeneity of the subsurface. In addition to that, the BHEs can be subject to further sources of uncertainty such as the thermal impact of underground infrastructures like underground car parks (Noethen et al., 2023a), clogged wells (Song et al., 2020), or interference with other subsurface thermal systems such as other active BHE fields or aquifer thermal energy storage systems (Noethen et al., 2023b). The mentioned examples have in common that their effect on the temperature changes in the ground cannot be explicitly captured by the FLS model (Eq. (1)). Instead, this is reflected by incorporating measured temperature changes in the sequential optimization (Eq. (10)). In case studies I and II, the maximum uncertainty range is up to 5 % and 7 %, respectively. These values that represent the descriptive uncertainty rates are multiplied by the increase or decrease of temperature from the previous time-step, $\overrightarrow{\Delta T}_{DU}(\Delta x_i,\Delta y_j,t_m)$, and added to the simulated value, $\overrightarrow{\Delta T}_{sim}(\Delta x_i,\Delta y_j,t_m)$, in order to generate the true temperature change. The temperature change caused by the excess load, $\overrightarrow{\Delta T}_{excess}$, is the other source of temperature variation that has to be included in the measured values. We can summarize the components of the measured temperature change by:

$$\overrightarrow{\Delta T}_{meas}\left(\Delta x_i,\Delta y_j,t_m\right)=\overrightarrow{\Delta T}_{sim}\left(\Delta x_i,\Delta y_j,t_m\right)+\overrightarrow{\Delta T}_{DU}\left(\Delta x_i,\Delta y_j,t_m\right)+\overrightarrow{\Delta T}_{excess}\left(\Delta x_i,\Delta y_j,t_m\right) \tag{11}$$

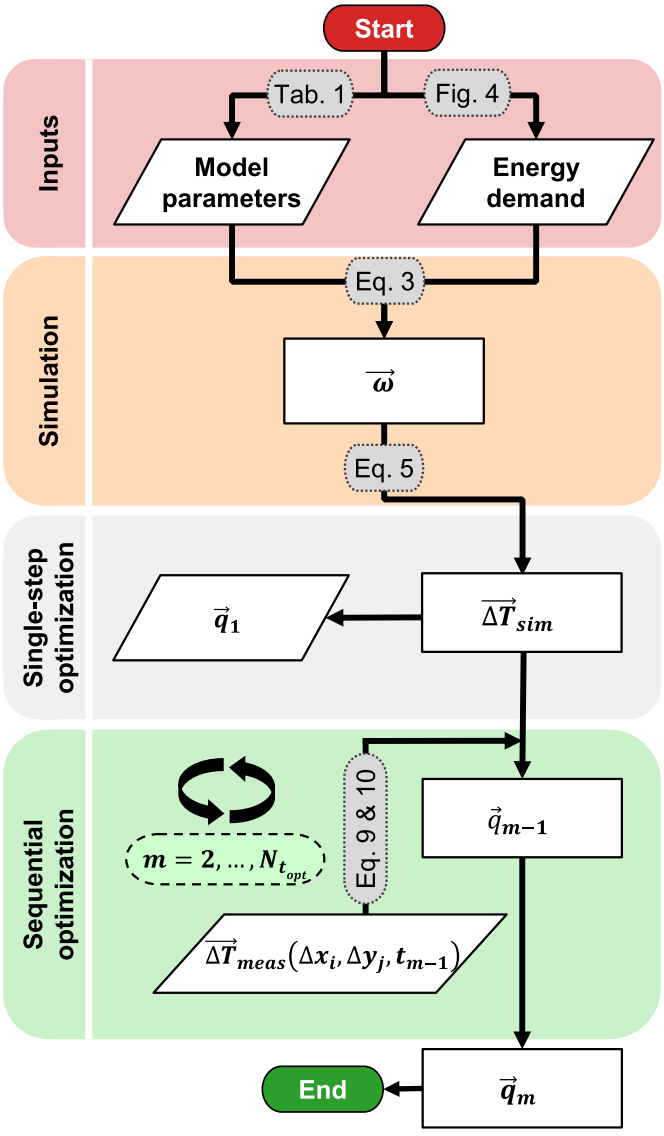

Fig. 2. Flowchart of the proposed method.

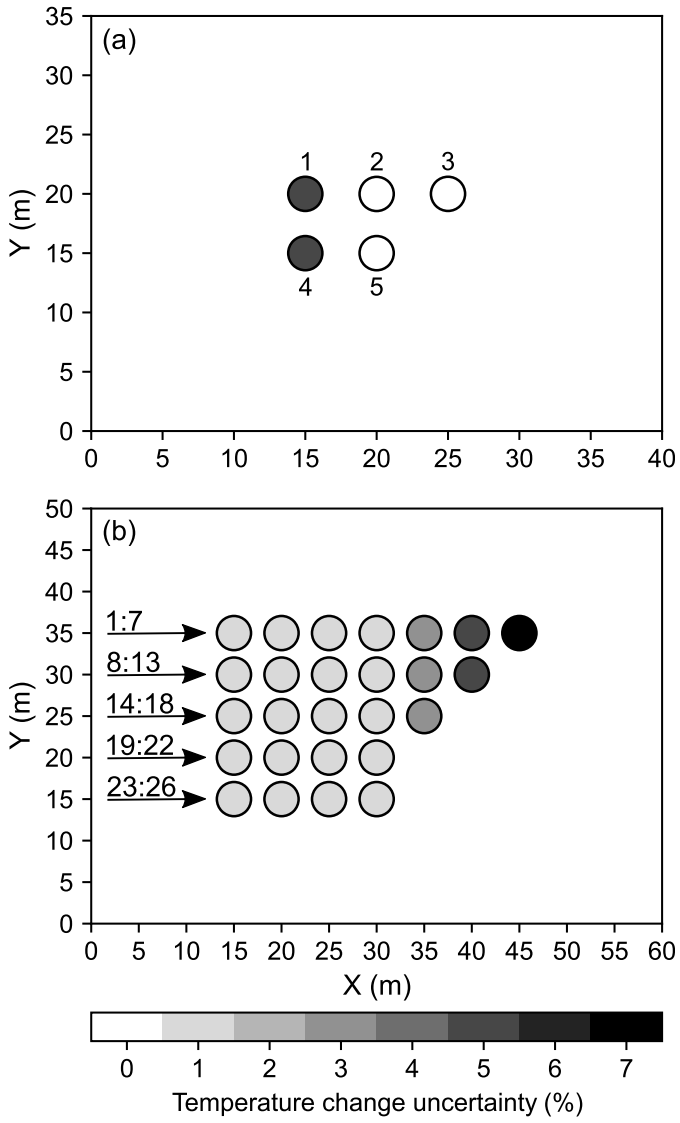

Fig. 3. Geometric layout of numbered BHEs of (a) case study I and (b) case study II. The numbers on the arrows in (b) indicate the index of the BHEs, from left to right, in each row of the array. These numbers are used to refer to each individual BHE.

Both hypothetical BHE fields are located at a site where the ground consists mainly of clay and silt. The subsurface is considered homogeneous with negligible groundwater flow. The values for the thermal properties are taken from the guidelines of the Association of German Engineers (VDI 2001), and the parameter specifications are listed in Table 1. Under the assumption that each individual borehole is 100 m long, the heat extraction rate per length is 24 W/m, and the annual operating time is 1,800 h (De Paly et al., 2012; VDI 2001). The total annual energy demands are 21.6 and 112.32 MWh for case study I and II, respectively.

This total energy demand is non-uniformly distributed over 12 months of the year, based on the assumption that the site is located in a country with Central European climate conditions and there is no heating demand during the summer months (June, July, and August). Even though the heating demand of consumers such as for space heating can be predicted, the true demand often varies significantly depending in particular on consumer behavior and climate variability. In order to account for this, our study considers a discrepancy between planned and actual energy demand in each month, the so-called excess load as shown in Fig. 4. The optimal workloads in this study are always calculated based on the predefined heating demand. At the end of each month, the current optimal load pattern is then scaled relatively to fulfill the surplus or shortfall load. Subsequently, the temperature change resulting from this over- or underload is calculated and applied as new knowledge in the next iteration of optimization. Sequential optimization gradually considers the deviation in the extracted load. Evidently, this cannot alter the past months, but it may be beneficial to modify the optimal patterns in the remainder of the operational lifetime. Here, as default it is assumed that the planned energy demand is always underestimated in comparison to the real demand.

Given the arrangement of the fields and the 180-month operation, this linear programming optimization problem for case study I and II covers 1,261 and 5,041 decision variables, composed of 900 loads, $\vec{q}$, along with 361 virtual variables, and 4,680 loads, $\overrightarrow{q}$, along with 361

Table 1
Parameter specifications for case studies.

Parameter	Value	Unit
Length of borehole, L	100	m
Thermal conductivity, λ	1.70	W m^{-1} K^{-1}
Thermal diffusivity, α	7.1 × 10^{-7}	m^2 s^{-1}

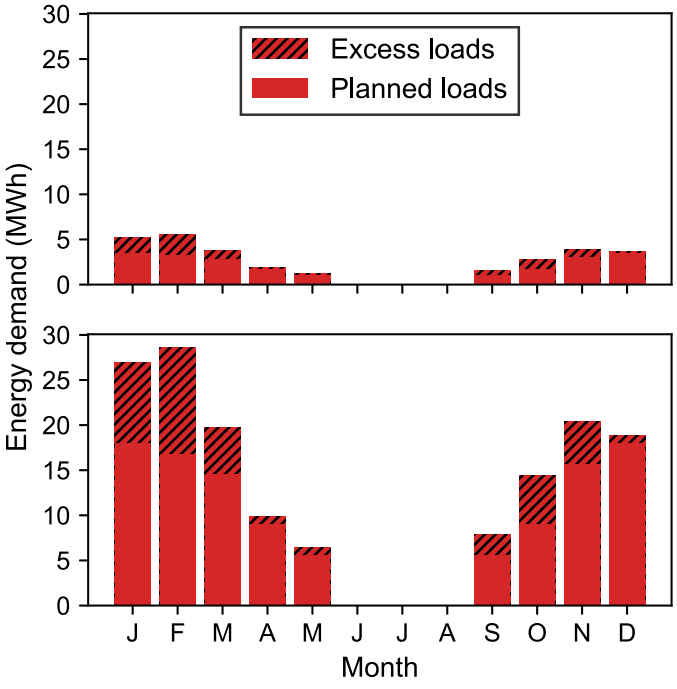

Fig. 4. Original monthly heat demand profile and the corresponding excess load for the case with (a) 5 BHEs and (b) 26 BHEs.

virtual variables, respectively. Aside from this, the formulations include 4,861 and 23,761 constraints associated with the five and 26 BHEs, respectively.

In the next section, the optimal load allocation patterns proposed by both optimization methods are assessed. The criterion for evaluating the efficiency of the optimization techniques is the maximum of imposed thermal anomaly in the ground at the end of the operating time by applying the proposed patterns. For both case studies, the distribution of subsurface temperature changes at 50 m depth are calculated. The mid-depth temperature is chosen in line with previous work (Bayer et al., 2014) and according to the suggestions by Zeng et al. (2002) to consider this temperature as a representative value for applications. However, any site-specific conditions or e.g. layered heterogeneity of ground properties may be accounted for by alternative models (Erol and François, 2018). To compare the performance of single-step and sequential optimization, we need to scale the proposed scenarios of single-step optimization, which is only possible at the end of the operational time in order to have equal amounts of extracted load. This means, the optimized BHE loads of the single-step optimization are increased or decreased relatively to match the realized heat demand. This is based on the assumption that the initially optimized relative load pattern is implemented, but depending on the true heat demand the overall load may need to be adjusted.

The circle colors in Fig. 3 indicate the assumed percentagewise deviation of the monthly temperature change compared to the simulated values for the given month due to the subsurface descriptive heterogeneity. So, the darker the color of BHEs, the higher the uncertainty.

3. Results and discussion

3.1. Maximum temperature change profiles

In this section, the maximum of the temperature changes during the operating time is presented in the cases where single-step and sequential optimization procedures are applied. As demonstrated for both configurations in Fig. 5, the resulting subsurface temperature changes by sequential optimization are significantly lower. The trend shows that in the first months of operation, there is no noticeable difference between the two optimization methods, but in the long run, the sequential outperforms the single-step method. There is an obvious benefit from the adaptive strategy underlying the sequential framework, where the subsurface temperature changes in the field are repeatedly measured during operation, and they are compared with the expected values at the end of each month. At each time step, the implemented deviation between simulated and measured data implies that we were not able to optimize the system perfectly in the last month, but we can react. Thus, there is an opportunity to avert cumulative deviations in the upcoming months. By measuring the thermal state of the ground each month, new initial thermal conditions can be used to revise the prediction of the model. This leads to a new starting point for the optimizer and to potentially different optimal load distributions for the remaining months. Fig. 5 reveals that the optimal patterns of the sequential variant result in lower temperature anomalies of about 2.9 K and 8.9 K in case study I and II, respectively, over the 15 years of operation. This means that the proposed approach leads to 27 % lower temperature changes in the case of five BHEs and 34 % lower temperature changes in the case of

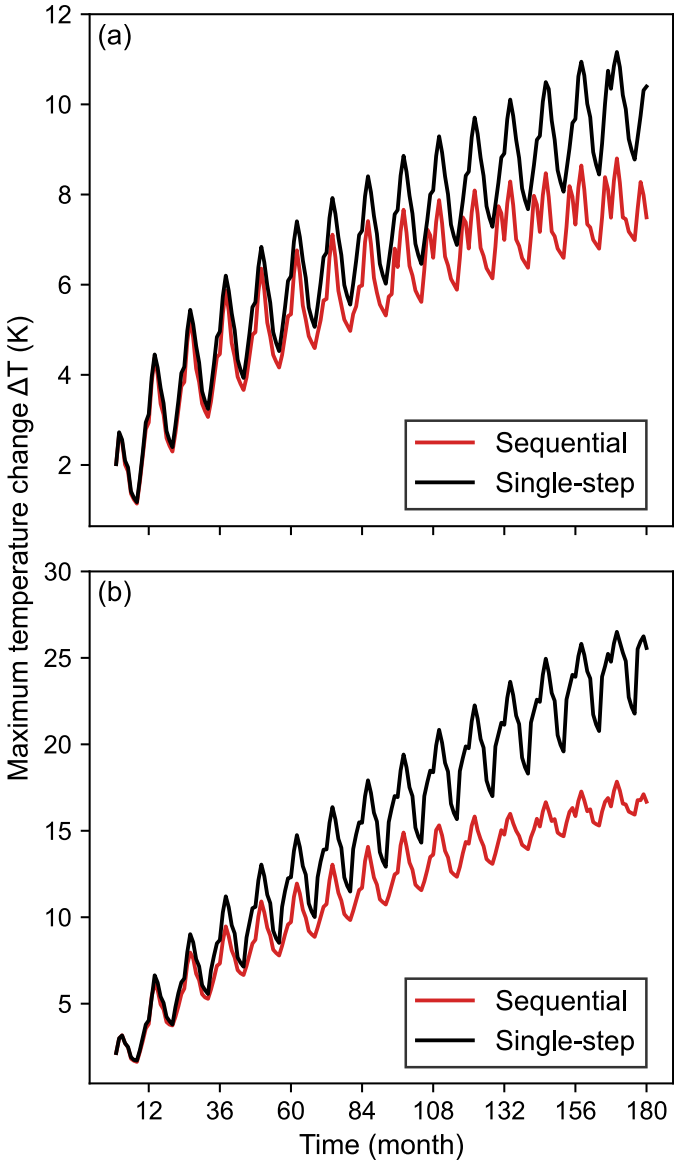

Fig. 5. Maximum of temperature change at 50 m depth over 15 operational years by using single-step and sequential optimization for (a) case study I and (b) case study II.

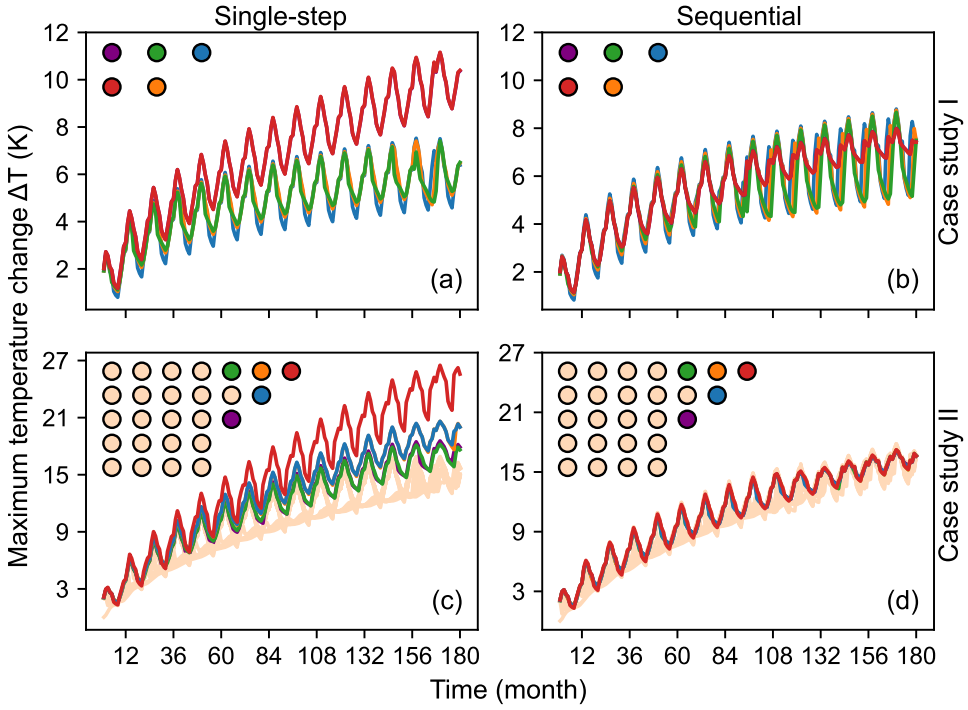

Fig. 6. Temperature change evolution of each single borehole at 50 m depth in the (a, b) five BHEs and (c, d) 26 BHE field using (a, c) single-step optimization and (b, d) sequential optimization. The pictogram at the top left of each plot shows the relative position of the BHEs in the field based on Fig. 3.

26 BHEs compared to the single-step optimization at the end of the 15 years of operation.

In Fig. 5, only the maximum temperature change of the BHE fields over time is shown. Note that this is the criterion of the objective function (Eq. (5)). However, for a more detailed insight into which BHE induces the maximum temperature change, Fig. 6 presents the temperature change evolution of each BHE individually for case study I and II. Obviously, in case study I the underestimation of the thermal effect of BHEs #1 and #4 (in accordance with Fig. 3a) is critical for the solution obtained by single-step optimization. Together with the uncertainties in the heating demand, the single-step solution does not react to deviations and there is an increasing local cooling at these boreholes in Fig. 6a. Fig. 6b demonstrates that the general characteristics and seasonal dynamics of the temperature variations for all BHEs are in a similar range in the sequential framework. In contrast, the optimizer responds properly and mitigates the local cooling effects at BHEs #1 and #4. This is compensated by higher loads for the other BHEs. Interestingly, the critical BHEs in the sequential optimization result (Fig. 6b) are other BHEs, the central BHEs #2, #3, and #5. This indicates that these BHEs have strongest interference with neighboring ones.

In a similar manner, the maximum temperature change in each borehole for case study II is calculated. For a better visual comparison in this dense case, only the imposed temperature change by critical BHEs are shown in different colors and the remaining BHEs with similar temperature change trend are not distinguished. Fig. 6c shows that neglect of subsurface heterogeneity at the position of BHE #7 and not considering the actual extracted energy again is unfavorable. A maximum temperature change in around seven years by single-step optimization is of the same order of magnitude as the maximum temperature change caused by sequential optimization in 15 years (Fig. 6d). Fig. 6 confirms that sequential optimization tends to result in a more uniform temperature change across the entire field, thereby compensating for the uncertainties in the prediction of the induced temperature changes and heating demand. In the case of five BHEs for the single-step optimization, the BHEs experience a temperature change in the range of about 6.2 to 10.5 K, while in the sequential optimization, the temperature change for all BHEs is approximately 7.5 K at the end of 15 years. In the case of 26 BHEs, the single-step optimization leads to temperature changes in the range of about 15.6 to 25.5 K, whereas the sequential optimization patterns restrict the temperature change for all BHEs to a tight range of about 17 K after 15 operational years.

3.2. *Optimal load patterns*

In this part, we present the distribution patterns of the optimal loads over the operating period resulting from the single-step as well as the sequential optimization for both case studies. The optimal load patterns of four time steps are shown exemplarily in Fig. 7 as a visual comparison of the load assignments by two methods. The single-step and sequential optimization propose an identical initial load distribution for both case studies, but over time they diverge from each other. In order to compare the different patterns, the values of the allocated loads on each individual borehole are divided by their length (100 m, Table 1) to derive a specific heat extraction rate, q. To simplify visual inspection, the intensity of the color and the size of the circles at the positions of the BHEs indicate the scale of load allocation to each particular BHE.

In an operating field with a similar configuration as case study I, if the thermal properties of the ground were fully known and there were no uncertainties, BHE #2 would be more likely to yield a more pronounced temperature anomaly in the subsurface than the others while this BHE is surrounded by the other BHEs that are actively operating. In the automatic optimal design of this field with the objective of minimizing the temperature change in the ground, the algorithm tends to reduce the assigned load on BHE #2 and distribute the excess load fairly evenly among the other BHEs. Fig. 7a shows that the single-step algorithm adopts a similar strategy in case study I. In contrast, the sequential algorithm recognizes that previous model predictions do not match the truth. Therefore, the algorithm learns and automatically modifies the previously proposed scenarios for upcoming months (Fig. 7b). It prevents local cooling by reducing the load of the BHEs where strong thermal anomalies have been created. It reduces the heat extraction of the poorly performing BHEs #1 and #4 and rather accentuates the role

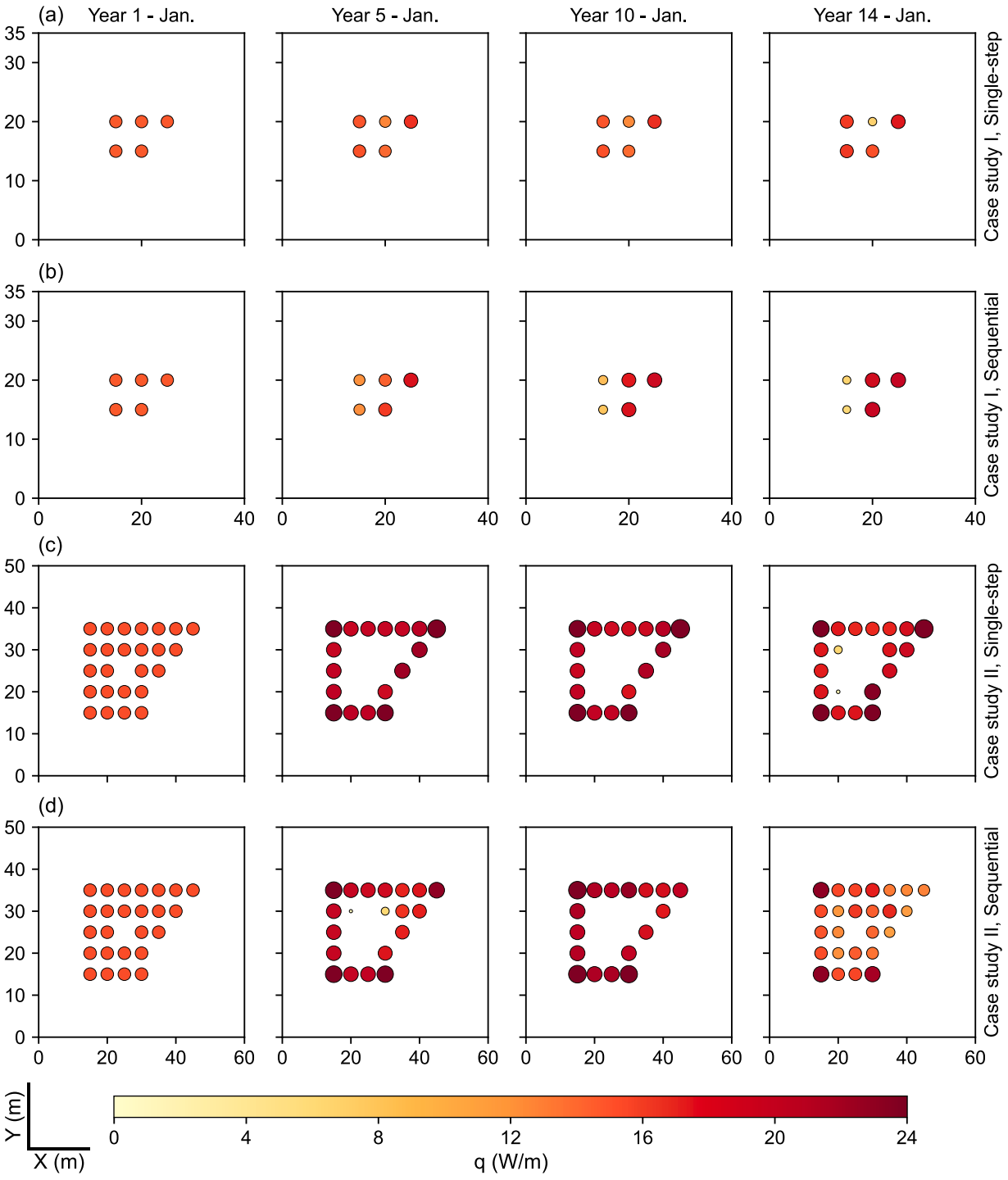

Fig. 7. The resulting optimal load patterns at some selected operating intervals that are obtained for case study I by using (row a) single-step optimization, (row b) sequential optimization and for case study II by using (row c) single-step optimization and (row d) sequential optimization. The darker the color and the larger the BHEs, the higher the heat extraction rate.

of other BHEs. This demonstrates that an underestimated temperature change of 5 % compared to the prediction by the analytical model each month already causes bad performance during long-term operation.

Fig. 7c shows that the single-step algorithm attempts to minimize the temperature change following the reasonable strategy of assigning the loads to the fringe of the field rather than to the inner part. As soon as the system is confronted with unexpected thermal behavior in these outer boreholes, this strategy no longer works. For example, BHE #7, which is located on the edge of the field, is susceptible to a higher level of uncertainty. Similar to case study I, the single-step optimization will not be informed of the gradual thermal evolution of the ground and thus causes a relatively strong local cooling here. This is avoided by the sequential procedure (Fig. 7d).

As the heat in the case examples of this study is transferred through conduction, the strongest thermal anomalies occur in the vicinity of the BHEs. Therefore, the uniformity of the thermal field is inversely proportional to the maximum temperature change. This is exemplified in the study by De Paly et al. (2012). Since the sequential optimization

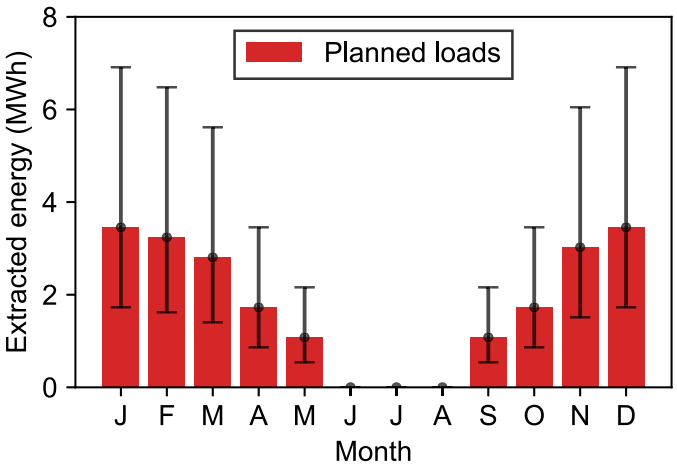

Fig. 8. Original heat demand profile with the corresponding uncertainty range.

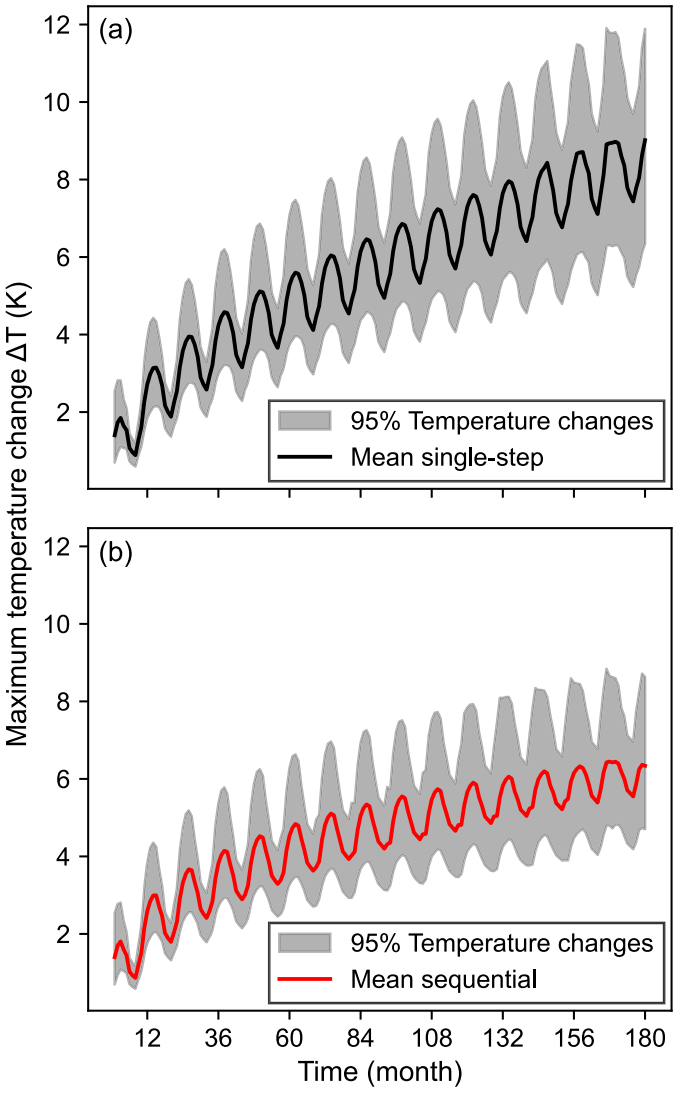

Fig. 9. Maximum temperature change at 50 m depth considering 10,000 distinct series of uncertainty in heating demand profile by using (a) single-step optimization (b) sequential optimization for case study I.

outperforms the single-step variant, it can be conceptually proven that the temperature field is much more uniform with sequential optimization.

3.3. Sensitivity analysis on the variability of heating demand

In the previous sections, the optimization procedure is applied assuming that the uncertainty in the heat demand is only due to an underestimation of the heat demand profile. Thus, as shown in Fig. 4, this means that we were dealing only with excess heating loads. To further evaluate the general applicability of the proposed approach, the performance of sequential optimization under various uncertainty patterns of heat demand is tested. For this purpose, a stochastic study case is defined where the heat demand in each month can be overestimated, underestimated, or experience no uncertainty. We consider the configuration of the BHEs in case study I to conduct this analysis. In order to investigate the sensitivity of the proposed optimization method to varying loads, 10,000 samples are taken from a normal distribution $\sim \mathcal{N}(0,\ 1)$. Each random sample provides a unique and new energy demand profile for the entire year that spans a differing range of uncertainty levels for each month. The optimizations, both the single-step and the sequential variants, are performed under the assumption that each random sample is a new heat demand that needs to be met. Error bars in Fig. 8 show that the range of uncertainty in heat demand can vary from −50 % to +100 % of the initially planned profile (red bars).

While all other scenario settings remain unchanged, each of these random samples is treated as an independent and unique energy demand profile for the optimization. Then, the maximum temperature change of each optimized sample is calculated over 15 operational years. A 95 % confidence interval in addition to the mean of all induced temperature changes by both optimization methods is shown in Fig. 9.

Fig. 9 shows even with this mixed combination of uncertainties in heat demand, the sequential method outperforms the single-step optimization by imposing on average a smaller maximum temperature change of about 2.7 K in the subsurface. This analysis guarantees that the proposed method is not tied to any particular mode or range of heating demand uncertainty. In addition, it can be stated that the seasonality of the temperature change dynamic can be captured by the proposed method in different ranges of the heat demand variations.

4. Conclusions

Our presented work builds upon existing concepts of individual load optimization of BHEs operated together in a field. The novelty is that observations during operation are utilized to restart load optimization. This sequential concept revises the operational mode to avoid local cooling in a field. This straightforward procedure is implemented to account for deficiencies in describing ground thermal processes. We introduced the compound effect of any influencing factors that cause inaccuracy in the performance prediction in the form of a BHE-specific temperature change uncertainty level. In addition to ground-related uncertainties, the implication of energy demand variability on the evolution of thermal conditions is considered.

The results of two case studies reveal that the flexibility of sequential optimization in acquiring new information and possibility of load pattern modifications is beneficial. The allocated load patterns proposed by sequential optimization lead to lower temperature anomalies of 2.9 K and 8.9 K for fields with five and 26 BHEs, respectively, over 15 years of operation compared to single-step optimization. The flexibility of our approach is in favor of extending the sustainable life of the system and alleviating negative environmental impacts by postponing the occurrence of the permissible maximum temperature change. In detail, the role of underestimation and overestimation of heating demand on the deterioration of optimized patterns is investigated. The advantage of the sequential optimization is demonstrated by the case studies with underestimated demand, and generally for fluctuations in heating

demand in the range of −50 % and up to +100 % of the planned loads in a stochastic framework. As a next step, it is also recommended to further develop the current methodology to a procedure that not only updates the thermal conditions as a modified initial point for re-optimization, but also revises model settings in order to reduce the prediction uncertainty during the course of operation. Furthermore, it is suggested that in addition to optimizing the heat load distribution, the efficiency of the ground source heat pumps could also be included in the objective function to achieve a more inclusive optimization framework for the entire system.

CRediT authorship contribution statement

Hesam Soltan Mohammadi: Conceptualization, Methodology, Software, Visualization, Writing – original draft. **Lisa Maria Ringel:** Methodology, Software, Writing – review & editing. **Michael de Paly:** Conceptualization, Software, Writing – review & editing. **Peter Bayer:** Conceptualization, Methodology, Writing – review & editing, Supervision, Funding acquisition.

Declaration of competing interest

The authors declare that they have no known competing financial interests or personal relationships that could have appeared to influence the work reported in this paper.

Data availability

Data will be made available on request.

Acknowledgments

This work was supported by the German Research Foundation (DFG) based on grant number BA2850/7–1. The authors thank Ryan Pearson, Wiebke Lehmann, and Lukas Römhild for proofreading, Christoph Bott for his help in improving the design of Fig. 1 and Fig. 2, and Hannes Hemmerle for helpful discussion on the design idea of the graphical abstract. The authors also appreciate helpful and constructive comments from two anonymous reviewers.

References

Abdelaziz, S.L., Ozudogru, T.Y., Olgun, C.G., Martin, J.R., 2014. Multilayer finite line source model for vertical heat exchangers. Geothermics 51, 406–416. https://doi.org/10.1016/j.geothermics.2014.03.004.

Antelmi, M., Turrin, F., Zille, A., Fedrizzi, R., 2023. A New Type in TRNSYS 18 for Simulation of Borehole Heat Exchangers Affected by Different Groundwater Flow Velocities. Energies 16 (3), 1288. https://doi.org/10.3390/en16031288.

Atam, E., Patteeuw, D., Antonov, S.P., Helsen, L., 2016. Optimal Control Approaches for Analysis of Energy Use Minimization of Hybrid Ground-Coupled Heat Pump Systems. IEEE Trans. Control Syst. Technol. 24, 525–540. https://doi.org/10.1109/TCST.2015.2445851.

Bayer, P., de Paly, M., Beck, M., 2014. Strategic optimization of borehole heat exchanger field for seasonal geothermal heating and cooling. Appl. Energy. 136, 445–453. https://doi.org/10.1016/j.apenergy.2014.09.029.

Beck, M., Hecht-Méndez, J., De Paly, M., Bayer, P., Blum, P., Zell, A., 2010. Optimization of the energy extraction of a shallow geothermal system. In: 2010 IEEE World Congr. Comput. Intell. WCCI 2010 - 2010 IEEE Congr. Evol. Comput. CEC 2010. https://doi.org/10.1109/CEC.2010.5585921.

Beck, M., Bayer, P., de Paly, M., Hecht-Méndez, J., Zell, A., 2013. Geometric arrangement and operation mode adjustment in low-enthalpy geothermal borehole fields for heating. Energy 49, 434–443. https://doi.org/10.1016/j.energy.2012.10.060.

Bernier, M.A., Pinel, P., Labib, R., Paillot, R., 2004. A multiple load aggregation algorithm for annual hourly simulations of GCHP systems. Hvac&R Res 10, 471–487.

Bidarmaghz, A., Narsilio, G.A., Johnston, I.W., Colls, S., 2016. The importance of surface air temperature fluctuations on long-term performance of vertical ground heat exchangers. Geomech. Energy Environ. 6, 35–44. https://doi.org/10.1016/j.gete.2016.02.003.

Blum, P., Menberg, K., Koch, F., Benz, S.A., Tissen, C., Hemmerle, H., Bayer, P., 2021. Is thermal use of groundwater a pollution? J. Contam. Hydrol. 239, 103791 https://doi.org/10.1016/j.jconhyd.2021.103791.

BniLam, N., Al-Khoury, R., 2020. Parameter identification algorithm for ground source heat pump systems. Appl. Energy. 264, 114712 https://doi.org/10.1016/j.apenergy.2020.114712.

Boban, L., Soldo, V., Fujii, H., 2020. Investigation of heat pump performance in heterogeneous ground. Energy Convers. Manag. 211, 112736 https://doi.org/10.1016/j.enconman.2020.112736.

Chen, S., Cai, W., Witte, F., Wang, X., Wang, F., Kolditz, O., Shao, H., 2021. Long-term thermal imbalance in large borehole heat exchangers array – A numerical study based on the Leicester project. Energy Build 231, 110518. https://doi.org/10.1016/j.enbuild.2020.110518.

Cimmino, M., Bernier, M., 2014. A semi-analytical method to generate g-functions for geothermal bore fields. Int. J. Heat Mass Transf. 70, 641–650. https://doi.org/10.1016/j.ijheatmasstransfer.2013.11.037.

Cimmino, M., Bernier, M., 2014. Effects of unequal borehole spacing on the required borehole length. ASHRAE Trans 120, 158.

Cimmino, M., Bernier, M., Adams, F., 2013. A contribution towards the determination of g-functions using the finite line source. Appl. Therm. Eng. 51, 401–412. https://doi.org/10.1016/j.applthermaleng.2012.07.044.

De Paly, M., Hecht-Méndez, J., Beck, M., Blum, P., Zell, A., Bayer, P., 2012. Optimization of energy extraction for closed shallow geothermal systems using linear programming. Geothermics 43, 57–65. https://doi.org/10.1016/j.geothermics.2012.03.001.

De Ridder, F., Diehl, M., Mulder, G., Desmedt, J., Van Bael, J., 2011. An optimal control algorithm for borehole thermal energy storage systems. Energy Build 43, 2918–2925. https://doi.org/10.1016/j.enbuild.2011.07.015.

Egidi, N., Giacomini, J., Maponi, P., 2023. Inverse heat conduction to model and optimise a geothermal field. J. Comput. Appl. Math. 423, 114957 https://doi.org/10.1016/j.cam.2022.114957.

Erol, S., François, B., 2014. Efficiency of various grouting materials for borehole heat exchangers. Appl. Therm. Eng. 70, 788–799. https://doi.org/10.1016/j.applthermaleng.2014.05.034.

Erol, S., François, B., 2018. Multilayer analytical model for vertical ground heat exchanger with groundwater flow. Geothermics 71, 294–305. https://doi.org/10.1016/j.geothermics.2017.09.008.

Eskilson, P., 1987. Thermal analysis of heat extraction boreholes.

Fascì, M.L., Lazzarotto, A., Acuña, J., Claesson, J., 2021. Simulation of thermal influence between independent geothermal boreholes in densely populated areas. Appl. Therm. Eng. 196. https://doi.org/10.1016/j.applthermaleng.2021.117241.

Gang, W., Wang, J., Wang, S., 2014. Performance analysis of hybrid ground source heat pump systems based on ANN predictive control. Appl. Energy. 136, 1138–1144. https://doi.org/10.1016/j.apenergy.2014.04.005.

Gehlin, S., 2002. Thermal response test: method development and evaluation (Doctoral dissertation, Luleå tekniska universitet).

Gil, A.G., Moreno, M.M., 2020. Current Legal Framework on Shallow Geothermal Energy Use in Spain. J. Sustain. Res. 2, 1–14. https://doi.org/10.20900/jsr20200005.

Gil, A.G., Schneider, E.A.G., Moreno, M.M., Cerezal, J.C.S., 2020. Shallow Geothermal Energy: Theory and Application. Springer Hydrogeology. https://doi.org/10.1007/978-3-030-92258-0.

Gultekin, A., Aydin, M., Sisman, A., 2016. Thermal performance analysis of multiple borehole heat exchangers. Energy Convers. Manag. 122, 544–551. https://doi.org/10.1016/j.enconman.2016.05.086.

Haehnlein, S., Bayer, P., Blum, P., 2010. International legal status of the use of shallow geothermal energy. Renew. Sustain. Energy Rev. 14, 2611–2625. https://doi.org/10.1016/j.rser.2010.07.069.

Hecht-Méndez, J., De Paly, M., Beck, M., Bayer, P., 2013. Optimization of energy extraction for vertical closed-loop geothermal systems considering groundwater flow. Energy Convers. Manag. 66, 1–10. https://doi.org/10.1016/j.enconman.2012.09.019.

Heim, E., Laska, M., Becker, R., Klitzsch, N., 2022. Estimating the Subsurface Thermal Conductivity and Its Uncertainty for Shallow Geothermal Energy Use—A Workflow and Geoportal Based on Publicly Available Data. Energies 15 (10), 3687. https://doi.org/10.3390/en15103687.

Hein, P., Kolditz, O., Görke, U.J., Bucher, A., Shao, H., 2016. A numerical study on the sustainability and efficiency of borehole heat exchanger coupled ground source heat pump systems. Appl. Therm. Eng. 100, 421–433. https://doi.org/10.1016/j.applthermaleng.2016.02.039.

Ikeda, S., Choi, W., Ooka, R., 2017. Optimization method for multiple heat source operation including ground source heat pump considering dynamic variation in ground temperature. Appl. Energy. 193, 466–478. https://doi.org/10.1016/j.apenergy.2017.02.047.

Lamarche, L., 2011. Analytical g-function for inclined boreholes in ground-source heat pump systems. Geothermics 40, 241–249. https://doi.org/10.1016/j.geothermics.2011.07.006.

Lazzarotto, A., Björk, F., 2016. A methodology for the calculation of response functions for geothermal fields with arbitrarily oriented boreholes - Part 2. Renew. Energy. 86, 1353–1361. https://doi.org/10.1016/j.renene.2015.09.057.

Lazzarotto, A., 2016. A methodology for the calculation of response functions for geothermal fields with arbitrarily oriented boreholes - Part 1. Renew. Energy. 86, 1380–1393. https://doi.org/10.1016/j.renene.2015.09.056.

Lee, C.K., 2011. Effects of multiple ground layers on thermal response test analysis and ground-source heat pump simulation. Appl. Energy. 88, 4405–4410. https://doi.org/10.1016/j.apenergy.2011.05.023.

Liu, W., Chen, G., Yan, B., Zhou, Z., Du, H., Zuo, J., 2015. Hourly operation strategy of a CCHP system with GSHP and thermal energy storage (TES) under variable loads: a case study. Energy Build 93, 143–153. https://doi.org/10.1016/j.enbuild.2015.02.030.

Lund, J.W., Boyd, T.L., 2016. Direct utilization of geothermal energy 2015 worldwide review. Geothermics 60, 66–93. https://doi.org/10.1016/j.geothermics.2015.11.004.
Lund, J.W., Toth, A.N., 2021. Direct utilization of geothermal energy 2020 worldwide review. Geothermics 90, 101915. https://doi.org/10.1016/j.geothermics.2020.101915.
Luo, J., Rohn, J., Bayer, M., Priess, A., Xiang, W., 2014. Analysis on performance of borehole heat exchanger in a layered subsurface. Appl. Energy. 123, 55–65. https://doi.org/10.1016/j.apenergy.2014.02.044.
Ma, Z., Xia, L., Gong, X., Kokogiannakis, G., Wang, S., Zhou, X., 2020. Recent advances and development in optimal design and control of ground source heat pump systems. Renew. Sustain. Energy Rev. 131 https://doi.org/10.1016/j.rser.2020.110001.
Marcotte, D., Pasquier, P., 2008. Fast fluid and ground temperature computation for geothermal ground-loop heat exchanger systems. Geothermics 37, 651–665. https://doi.org/10.1016/j.geothermics.2008.08.003.
Marcotte, D., Pasquier, P., Sheriff, F., Bernier, M., 2010. The importance of axial effects for borehole design of geothermal heat-pump systems. Renew. Energy. 35, 763–770. https://doi.org/10.1016/j.renene.2009.09.015.
Michopoulos, A., Kyriakis, N., 2009. A new energy analysis tool for ground source heat pump systems. Energy Build 41, 937–941. https://doi.org/10.1016/j.enbuild.2009.03.017.
Nguyen, A., Pasquier, P., Marcotte, D., 2017. Borehole thermal energy storage systems under the influence of groundwater flow and time-varying surface temperature. Geothermics 66, 110–118. https://doi.org/10.1016/j.geothermics.2016.11.002.
Noël, A., Cimmino, M.. Development of a topology optimization method for the design of ground heat exchangers. https://doi.org/10.22488/okstate.22.000017.
Noethen, M., Hemmerle, H., Menberg, K., Epting, J., Benz, S.A., Blum, P., Bayer, P., 2023a. Thermal impact of underground car parks on urban groundwater. Sci. Total Environ. 903, 166572 https://doi.org/10.1016/j.scitotenv.2023.166572.
Noethen, M., Hemmerle, H., Bayer, P., 2023b. Sources, intensities, and implications of subsurface warming in times of climate change. Crit. Rev. Environ. Sci. Technol. 53, 700–722.
Pasquier, P., Zarrella, A., Marcotte, D., 2019. A multi-objective optimization strategy to reduce correlation and uncertainty for thermal response test analysis. Geothermics 79, 176–187. https://doi.org/10.1016/j.geothermics.2019.02.003.
Perego, R., Dalla Santa, G., Galgaro, A., Pera, S., 2022. Intensive thermal exploitation from closed and open shallow geothermal systems at urban scale: unmanaged conflicts and potential synergies. Geothermics 103, 102417. https://doi.org/10.1016/j.geothermics.2022.102417.
Previati, A., Crosta, G., 2024. On groundwater flow and shallow geothermal potential: a surrogate model for regional scale analyses. Sci. Total Environ. 912, 169046 https://doi.org/10.1016/j.scitotenv.2023.169046.
Raymond, J., Lamarche, L., 2013. Simulation of thermal response tests in a layered subsurface. Appl. Energy. 109, 293–301. https://doi.org/10.1016/j.apenergy.2013.01.033.
Rivera, J.A., Blum, P., Bayer, P., 2017. Increased ground temperatures in urban areas: Estimation of the technical geothermal potential. Renewable Energy 103, 388–400. https://doi.org/10.1016/j.renene.2016.11.005.
Shoji, Y., Katsura, T., Nagano, K., 2023. Improvement of accuracy with uncertainty quantification in the simulation of a ground heat exchanger by combining model prediction and observation. Geothermics 107, 102611. https://doi.org/10.1016/j.geothermics.2022.102611.
Signorelli, S., Bassetti, S., Pahud, D., Kohl, T., 2007. Numerical evaluation of thermal response tests. Geothermics 36, 141–166. https://doi.org/10.1016/j.geothermics.2006.10.006.
Song, W., Liu, X., Zheng, T., Yang, J., 2020. A review of recharge and clogging in sandstone aquifer. Geothermics 87, 101857. https://doi.org/10.1016/j.geothermics.2020.101857.
Spitler, J.D., Gehlin, S.E.A., 2015. Thermal response testing for ground source heat pump systems - An historical review. Renew. Sustain. Energy Rev. 50, 1125–1137. https://doi.org/10.1016/j.rser.2015.05.061.
Spitler, J.D., Cook, J.C., Liu, X., 2020. A Preliminary Investigation on the Cost Reduction Potential of Optimizing Bore Fields for Commercial Ground Source Heat Pump Systems, 45th Work. Geotherm. Reserv. Eng. 1–13.
Spitler, J.D., West, T., Liu, X., 2022. Ground heat exchanger design tool with rowwise placement of boreholes. doi:10.22488/okstate.22.000016.
Stauffer, F., Bayer, P., Blum, P., Giraldo, N.M., Kinzelbach, W., 2013. Thermal Use of Shallow Groundwater. CRC Press.
Tsagarakis, K.P., Efthymiou, L., Michopoulos, A., Mavragani, A., Anđelković, A.S., Antolini, F., Bacic, M., Bajare, D., Baralis, M., Bogusz, W., Burlon, S., Figueira, J., Genç, M.S., Javed, S., Jurelionis, A., Koca, K., Ryżyński, G., Urchueguia, J.F., Žlender, B., 2020. A review of the legal framework in shallow geothermal energy in selected European countries: need for guidelines. Renew. Energy. 147, 2556–2571. https://doi.org/10.1016/j.renene.2018.10.007.
VDI, 2001. Thermal Use of the Underground. Part 2: Geothermal Heat Pump Systems: VDI 4640, Düsseldorf. VDI-Verlag, Düsseldorf, p. 43.
Wagner, V., Bayer, P., Kübert, M., Blum, P., 2012. Numerical sensitivity study of thermal response tests. Renew. Energy. 41, 245–253. https://doi.org/10.1016/j.renene.2011.11.001.
Yavuzturk, C., Spitler, J.D., 2000. Comparative study of operating and control strategies for hybrid ground-source heat pump systems using a short time step simulation model. Ashrae Trans 106, 192.
Yoshioka, M., Shrestha, G., Widiatmojo, A., Uchida, Y., 2022. Seasonal changes in thermal process based on thermal response test of borehole heat exchanger. Geothermics 102, 102390. https://doi.org/10.1016/j.geothermics.2022.102390.
Zanchini, E., Lazzari, S., Priarone, A., 2012. Long-term performance of large borehole heat exchanger fields with unbalanced seasonal loads and groundwater flow. Energy 38, 66–77. https://doi.org/10.1016/j.energy.2011.12.038.
Zeng, H.Y., Diao, N.R., Fang, Z.H., 2002. A finite line-source model for boreholes in geothermal heat exchangers. Heat Transf. - Asian Res. 31, 558–567. https://doi.org/10.1002/htj.10057.
Zhang, H., Han, Z., Ji, M., Li, G., Cheng, X., Yang, Z., Yang, L., 2021. Analysis of influence of pipe group arrangement and heat exchanger type on operation performance of the ground source heat pump. Geothermics 97, 102237. https://doi.org/10.1016/j.geothermics.2021.102237.
Zhang, C., Lu, J., Wang, X., Xu, H., Sun, S., 2022. Effect of geological stratification on estimated accuracy of ground thermal parameters in thermal response test. Renew. Energy. 186, 585–595. https://doi.org/10.1016/j.renene.2022.01.024.
Zhou, Z., Wu, S., Du, T., Chen, G., Zhang, Z., Zuo, J., He, Q., 2016. The energy-saving effects of ground-coupled heat pump system integrated with borehole free cooling: a study in China. Appl. Energy. 182, 9–19. https://doi.org/10.1016/j.apenergy.2016.07.124.